Investigation of optical and dispersion parameters of polyacrylonitrile (PAN) nanofibers fabricated via electrospinning method

K. DİNCER[a], G. ÖNAL[a], Ü. AKIN[b], N. TUĞLUOĞLU[c], Ö. F. YÜKSEL[b,*]
[a]*Department of Mechanical Engineering, Faculty of Engineering and Natural Sciences, Konya Technical University, Konya, Turkey*
[b]*Department of Physics, Faculty of Science, Selçuk University, Konya, Turkey*
[c]*Department of Energy Systems Engineering, Faculty of Engineering, Giresun University,Giresun, Turkey*

The current paper deals with the studies of optical properties of Polyacrylonitrile (PAN) nanofibers, as an engineering material with increasing technological attention. The optical properties of PAN nanofibers deposited by the electrospinning technique were investigated. We have introduced the dispersion and optical parameters of PAN nanofibers using a UV-Vis-NIR spectrophotometer. The morphologies of PAN nanofibers were observed by scanning electron microscopy (SEM). The optical energy gap of PAN nanofibers was determined as 3.55 eV. In addition, the optical conductivity of PAN nanofibers was interpreted using the analysis of optical dielectric constants. The obtained results of PAN nanofiber help the desirable property for optoelectronic devices.

(Received October 22, 2020; accepted November 24, 2021)

Keywords: PAN nanofiber, UV-Vis-NIR spectrum, Electrospinning, Dispersion parameters, Optical constants, Optical band gap

1. Introduction

One of the most efficient and most developed formation processes of allowing to obtain high-quality nanofibers is the electrospinning method [1-2]. Electrospinning, a type of the powerful techniques to handle polymers into continual fibers with diameters ranging from micrometers to nanometers, has attracted important interest in a host of fields [3-6]. Zhang et al. [3] demonstrated that electrical conductive nanocomposite fibers were prepared with polyacrylonitrile (PAN) using the electrospinning method. Mack et al. [7] investigated the elastic properties of nanoplatelet/PAN nanocomposite fibrils using the electrospinning method. Ko et al. [8] used electrospinning to produce carbon nanotube reinforced spider silk. The electrospinning method was also used by Dincer et al. [9] to process activated carbon nanofiber (ACNF) layers.

For commercial carbon fibers, PAN is one of the best precursors due to its ability to produce fibers with high tensile strength and its high carbon yield [10-13]. Most PAN-based carbon fibers were used in aerospace applications [14], the textile industry [15], and composite technology [16]. Wang et al. [17] prepared carbon nanofibers from carbonizing electrospun PAN nanofibers and investigated their conductivity and structure. Gu and coworkers [18] have obtained PAN nanofibers as a precursor of carbon nanofibers with diameters in the range from 130 to 280 nm by electrospinning of PAN/DMF solution. They have studied the thermal properties and the morphologies and structures of electrospun PAN nanofibers. Park et al. [19] have produced carbon fibers by the electrospinning method and tide over the problems of fragile features of pitch-based carbon fibers.

To the best of our knowledge, there is no report on the dielectric, dispersion, and optical properties of PAN nanofibers prepared with the electrospinning method to adapt to optoelectronic applications. The goal of this work was to produce PAN nanofibers by electrospinning the solution and to investigate for the first time its optical and dispersion parameters for optical device applications. For this purpose, PAN nanofibers as a precursor of nanofibers with sizes in the range of 250 to 350 nm were obtained by electrospinning. Scanning electron microscopy (SEM) and UV-Vis-NIR spectrophotometer techniques for the prepared PAN nanofibers were used for the surface morphology and the calculation of optical and dispersion parameters, respectively. The optical energy gap of PAN nanofibers was estimated.

2. Experimental

2.1. Materials and Electrospinning of PAN nanofibers

Polyacrylonitrile (PAN purity 99 %, Mw = 150 000 g/mol) and N,N-dimethylformamide (DMF, 99.8%) were purchased from Sigma-Aldrich. PAN and DMF were used to make an 8 wt.%. The solution has been stirred by a constant at 90°C for 1h. The chosen spinning parameters for this study are listed in Table 1. The precursor mats have been spun under a relative humidity of 10–20% at room temperature. The electrospinning experimental setup is

given in Fig. 1. The fibers are collected on the aluminum foil in the form of non-woven fabric

Table 1. Electrospinning parameters for PAN electrospinning process

Processing parameters			
Feed rate (cc/h)	Applied voltage (kV)	Tip to collector (cm)	Collector rotational speed (rpm)
2	20	12	125

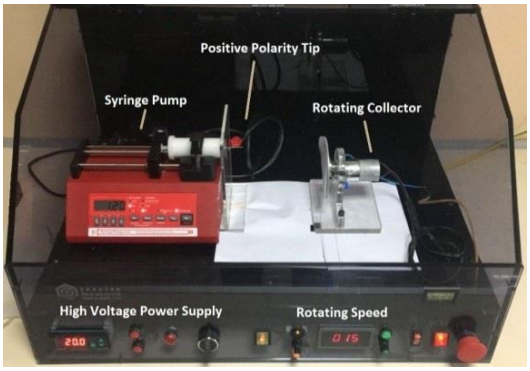

Fig. 1. Electrospinning experimental setup (color online)

2.2. Morphologies of electrospun PAN nanofibers

The surface morphology of the nanofibers was observed by scanning electron microscopy (Hitachi, S-4700). Figs. 2 a and b show the electrospun fibers prepared from 8 wt.% PAN/DMF solution at 20 kV with a tip-to-collector distance of 12 cm. PAN nanofibers with a diameter in the range of 250-350 nm were obtained Furthermore, the morphology of PAN nanofibers indicated that these measured fibers are debarred from structural defects and are defined by a homogeneous thickness along the whole length (Fig. 2a). Fig. 2c shows the cross-section of PAN nanofibers in the thickness of 1.322 µm. Optical absorption measurement of the PAN nanofibers is collected from a UV–Vis–NIR spectrophotometer (JASCO-V-670) in the wavelength range of 200-2000 nm. Dadvar et al. [20] reported that PAN nanofibers with diameters 197 nm and 321 nm indicated a small absorption in the UV-A region (315–400 nm) and UV-B region (280–315 nm), respectively.

3. Results and discussion

3.1. Transmission and reflection characterizations of PAN nanofibers

In order to analyze the optical properties of PAN nanofiber layer, which is assumed to be homogeneous with a uniform thickness, the transmittance (T) and reflectance (R) characteristics were measured for the produced layers, the spectra obtained are shown in Fig. 3. The transmittance (T) and reflectance (R) characteristics of the PAN nanofiber layer can be defined by the following relations [9,21]:

$$T = \frac{(1-R)^2 e^{-\alpha d}}{1-R^2 e^{-2\alpha d}} \quad (1)$$

and

$$R = \left(\frac{(n-1)^2+k^2}{(n+1)^2+k^2}\right) \quad (2)$$

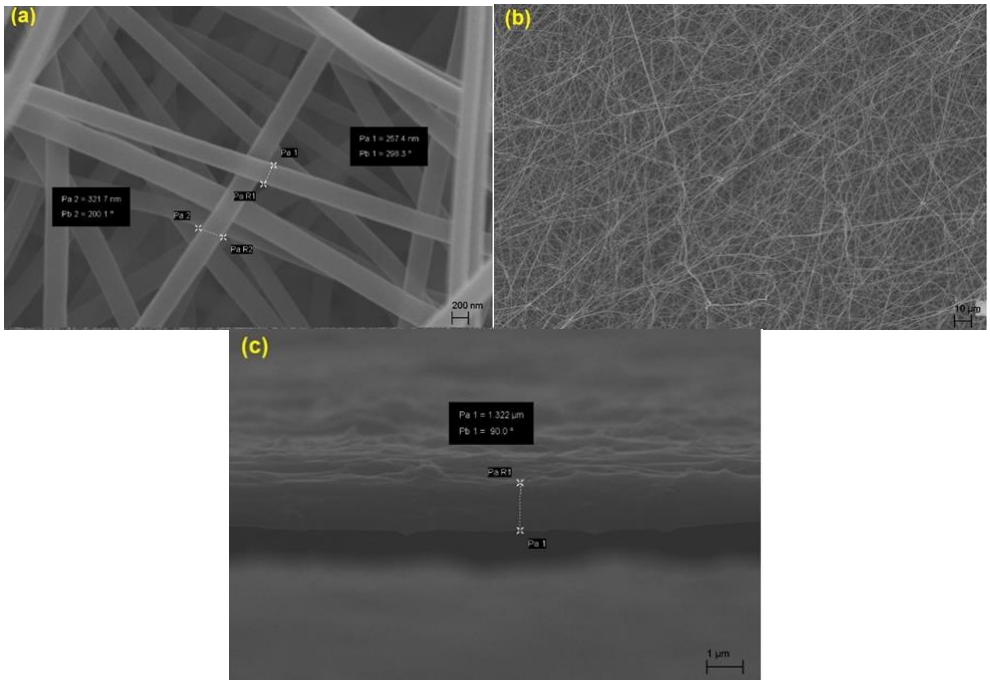

Fig. 2. SEM images showing the morphology of PAN nanofibers a) and b) the electrospun fibers c) the cross-section of PAN nanofibers

where d is the thickness, n is the refractive index, k and α are the extinction and the absorption coefficient, respectively. As observed from Fig. 3, the average values of the optical transmittance and reflectance have been determined for the visible region (400–700 nm) and changed from 1.17 to 18.84% and from 41.11 to 31.71%, respectively. Dincer et al. [9] have produced the activated carbon nanofiber (ACNF) layers via electrospinning. They have researched the optical properties of ACNF layer via UV–Vis-NIR spectrophotometer. It was found changing from 5.577 to 5.992% for T and from 3.883 to 4.657% for R. The graphene oxide and reduced graphene oxide (r-GO) have prepared using modified Hummer's technique by Khan et al. [22]. They have investigated their optical and electrical properties. The transmittance of r-GO has about 70%. This nature of r-GO can be used in the create of transparent electrode substance in solar cell applications.

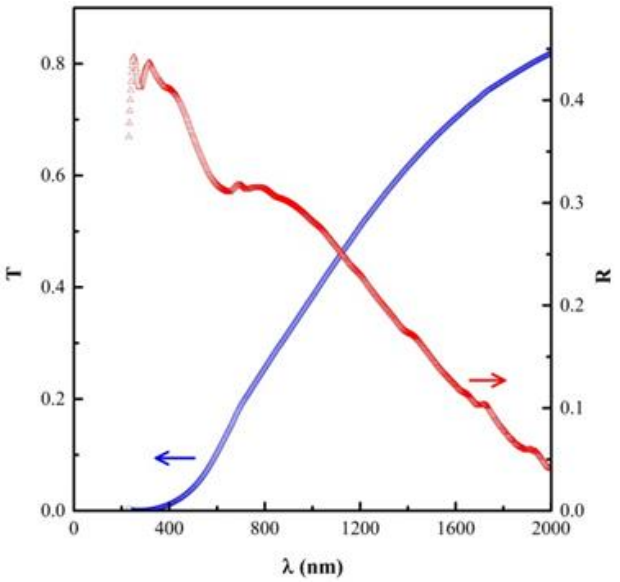

Fig. 3. The variation of optical transmittance and reflectance spectra with wavelenght of PAN nanofibers (color online)

3.2. Energy band gap calculation of PAN nanofibers

The transmittance and reflactance measurements have been taken out using an UV–Vis–NIR spectrophotometer in order to find the optical energy band gap value of the PAN nanofiber layer. The absorption coefficient (α) and optical band gap (E_g) of the produced nanofiber layer are calculated from the observed absorbance and transmittance values using the following relations [23-26].

$$\alpha = \frac{1}{d} ln \frac{(1-R)^2}{T} \tag{3}$$

$$(\alpha h\upsilon)^2 = B\left(h\upsilon - E_g\right) \tag{4}$$

where B is energy-independent constant, d is the thickness of the film, α is the absorption coefficient in cm^{-1} and $h\upsilon$ is photon energy. The thickness of PAN layer is determined as 1.322 μm by means of a profilometer. A plot of photon energy $(h\upsilon)$versus $(\alpha h\upsilon)^2$ drawn for PAN nanofiber layer produced is illustrated in Fig. 4. An analysis of absorption spectrum in the energy range from 0.5 eV to 4.5 eV shows that α follows the relation. The linear portion of the curve is extrapolated to the energy axis (x-axis) which is illustrated in Fig. 4. The intersection point gives the band gap energy of the PAN nanofiber. The estimated value of optical band gap energy found for PAN nanofiber is otained as 3.55 eV. Not only the band gap does give the optical band structure of the PAN layer, but also it reflects the basic absorption limit of the PAN layer [27-29]. Matysiak et al. [30] have reported the width of energy gap for PAN nanofibres as 3.465 eV. Dincer et al. [9] have reported that the band gap energy (E_g) of the activated carbon nanofiber (ACNF) layers produced using electrospinning is about 1.07 eV. The optical band gap of reduced graphene oxide (r-GO) fabricated by Khan et al. [22] is 4 eV.

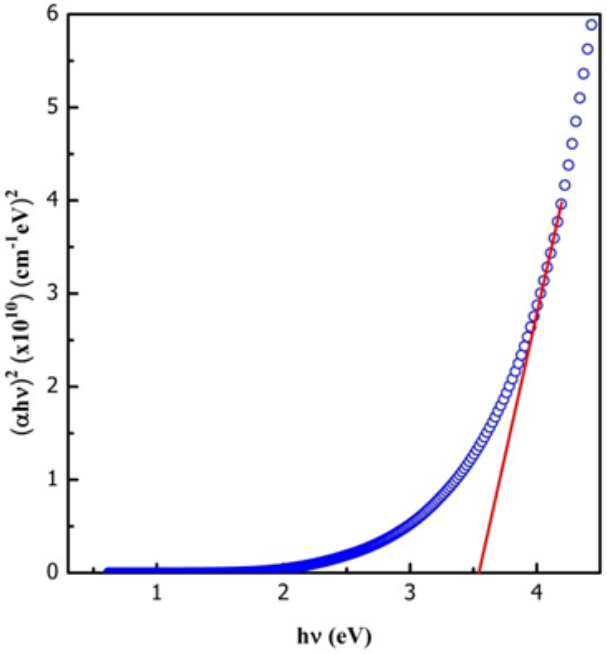

Fig. 4. The variation of $(h\upsilon)$ dependence of $(\alpha h\upsilon)^2$ of PAN nanofibers (color online)

3.3. Determination of refractive index (n) and extinction coefficient (k) of PAN nanofibers

According to the theory of reflectivity of light, the values of extinction coefficient (k) and refractive index (n) have been obtained by using the following equations [31,32]:

$$k = \frac{\alpha\lambda}{4\pi} \tag{5}$$

and

$$n = \left(\frac{1+R}{1-R}\right) + \sqrt{\frac{4R}{(1-R)^2} - k^2} \tag{6}$$

In order to determine the *n* and *k* values of the produced PAN nanofiber, the transmittance (*T*) and reflectance (*R*) were measured for the PAN nanofiber as can be seen Fig. 3, the spectra obtained for *n* and *k* are shown in Fig. 5. From Fig. 5, both the refractive index and the extinction coefficient of the PAN nanofibers first increases with increase in the wavelength and then decreases with further increase in the wavelength. Dincer et al. [9] have observed a very different behavior for the activated carbon nanofiber (ACNF) layers. The spectrum of *n* of PAN nanofibers is characterized by the presence of two peaks at about 250 nm (*n* = 4.696) and 314 nm (*n*= 4.893) while the *k* spectrum has a peak at about 274 nm (*k* = 0.123). The extinction coefficient decreases sharply from 300 to 1200 nm. The *n* and *k* values change 4.815-2.846 and 0.109-0.011 using between 300-1200 nm, respectively. Dincer et al. [9] reproted that the values of *k* and *n* change 0.0158-0.0268 and 1.492-1.550 via UV-Vis region (400-700 nm), respectively. The values of the refractive index (*n*) of and extinction coefficient (*k*) of the monolayer graphene film prepared by Mahmoud et al. [33] were determined to be 2.75-3.00 and 3.05-2.85 between 200 and 700 nm, respectively.

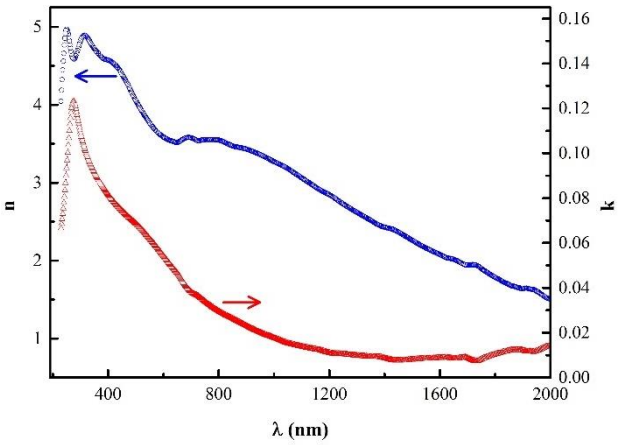

Fig. 5. The variation of refractive index (n) and extinction coefficient (k) with wavelength of PAN nanofibers (color online)

3.4. Urbach energy analysis of PAN nanofibers

The absorption tail of the PAN nanofibers is analyzed from Eq. (7).

$$\alpha = \alpha_0 \, exp\left(\frac{h\upsilon}{E_U}\right) \tag{7}$$

where $h\upsilon$ is photon energy, α_0 is a constant and E_U is the band tail width; the absorption coefficient is introduced by the so-called Urbach rule [34]. The Urbach rule defines the transition of optical between the occupied states in the valence band tail to the unoccupied states of the conduction band edge [34, 35]. The spectrum obtained of $ln(\alpha)$ versus photon energy $(h\upsilon)$ for PAN nanofiber is shown in Fig. 6. The value of E_U is calculated to be 0.335 eV from the slope of the spectrum. In addition, the steepness parameter, $\beta = kT/E_U$; is also determined as 0.074 for T = 300 K. Dincer et al. [9] reported that the value of E_U of ACNF layer has been determined to be 3.92 eV. The E_U value of the graphene oxide (r-GO) fabricated by Khan et al. [22] is 0.202 eV. The determined E_U for the graphene oxide (r-GO) is lower than it calculated both PAN nanofiber and ACNF layer.

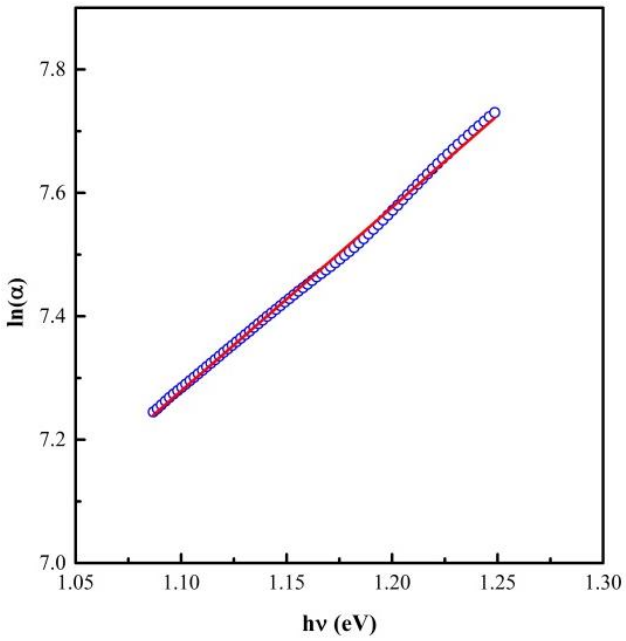

Fig. 6. Plot of $ln(\alpha)$ versus photon energy $(h\upsilon)$ for PAN nanofibers (color online)

3.5. Optical dispersion parameters of PAN nanofibers

Optical dispersion parameters of the any solid or thin films are noticeable due to play a significant act in making of the optical devices. The dispersion in refractive index can be assigned by the single-oscillator model offered by Wemple and Didomenico [36, 37]. Clearly, this model could not only be applied to define the optical properties in visible region for the materials or films, but also to assign some of their structural properties [38-40]. It is determined the dispersion energy (E_d) and single oscillator energy (E_0) according to this model [36,37]. The spectral dependence of the refractive index (*n*) is characterized by the equation [35-39]:

$$(n^2 - 1)^{-1} = \frac{E_0}{E_d} - \frac{1}{E_0 E_d}(h\upsilon)^2 \tag{8}$$

A plot of $(n^2 - 1)^{-1}$ versus $(h\upsilon)^2$ would be linearly fitted and would give the values of E_d and E_0 from the intercept of the y-axis (E_0/E_d) and the slope $(1/E_0E_d)$. Typical curve for PAN nanofiber is plotted in Fig. 7. Both E_d and E_0 values are calculated to be 27.09 eV and 3.5 eV, respectively. The values of E_0 and E_d of ACNF layer prepared by Dincer et al. [9] are found to be 7.269 eV and 7.549 eV, respectively. The dispersion energy and oscillator energy of the monolayer graphene film prepared by

Mahmoud et al. [33] were found to be E_d = 1.7 eV and E_0 = 3.1 eV, respectively.

A simple connection between the single-oscillator parameters of E_0 and E_d can be described in terms of moments of the imaginary part of the optical spectrum M_{-1} and M_{-3} as follows [41]:

$$E_0^2 = \frac{M_{-1}}{M_{-3}} \quad \text{and} \quad E_d^2 = \frac{M_{-1}^3}{M_{-3}} \tag{9}$$

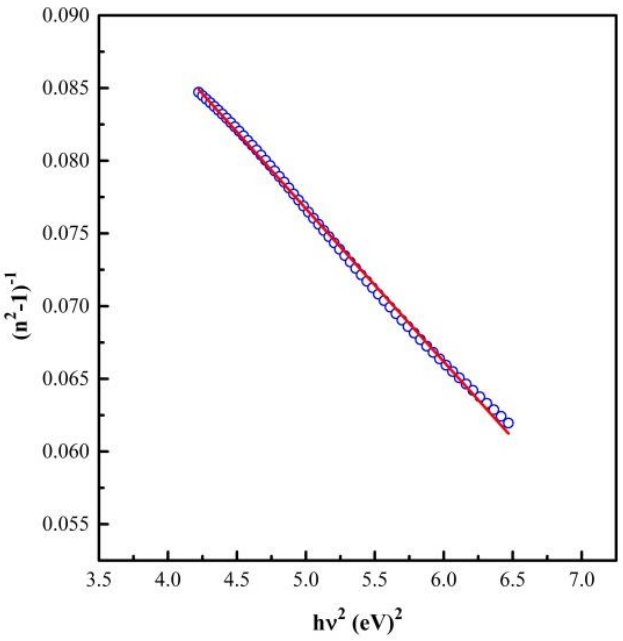

Fig. 7. The variation of $(n^2-1)^{-1}$ versus $(h\upsilon)^2$ of PAN nanofibers (color online)

The M_{-1} and M_{-3} moment values of PAN nanofiber are calculated as 7.74 and 0.632 eV^2 according to Eq. (9). In addition, the oscillator strength (*f*) is introduced by Wemple and Didomenico as [36]:

$$f = E_0 E_d \tag{10}$$

For PAN nanofiber, the oscillator strength (*f*) is determined as 94.82 eV^2.

The relation between refractive index *n*, the refractive index for infinite wavelength n_∞ and wavelength λ can be defined [36,37]:

$$\frac{n_\infty^2-1}{n^2-1} = 1 - \left(\frac{\lambda_0}{\lambda}\right)^2 \tag{11}$$

Fig. 8 illustrates the variation of $(n^2-1)^{-1}$ as a function of λ^{-2} for PAN nanofiber. The results show that the $\varepsilon_\infty = n_\infty^2$ and λ_0 values of PAN nanofiber are 11.55 and 1212.47 nm, respectively. For ACNF layer prepared by Dincer et al. [9], The $\varepsilon_\infty = n_\infty^2$ and λ_0 values have been found as 2.028 nm and 175.24 nm, respectively.

The changing of refractive index with wavelength can be rearranged by the following equation [36,37]:

$$n^2 - 1 = \frac{S_0 \lambda_0^2}{1-(\lambda_0/\lambda)^2} \tag{12}$$

where S_0 is the strength of average oscillator, $S_0 = (n_\infty^2 - 1)/\lambda_0^2 = E_d/E_0\lambda_0^2$, λ_0 is an the average oscillator wavelength. The result gives that the S_0 value of PAN nanofiber is 9.33 x 10^{-7} nm^{-2}. The value of S_0 for ACNF layer prepared by Dincer et al. [9] has been found as 3.35 x 10^{13} m^{-2}.

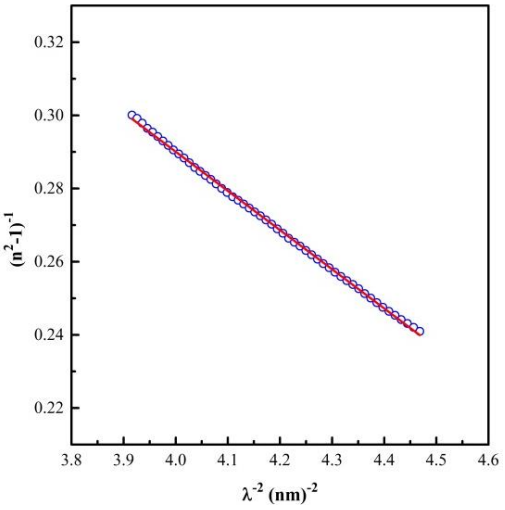

Fig. 8. The variation of $(n^2-1)^{-1}$ versus λ^{-2} of PAN nanofibers (color online)

3.6. Dielectric characterizations of PAN nanofiber

$\varepsilon^* = (\varepsilon_1 + i\varepsilon_2)$ is a significant quantity for desinging in extremely productive optoelectronic devices [42]. The real and imaginary part of the complex permittivity frequently characterizes the dielectric constant and the dielectric loss, respectively. The dielectric constant and loss is a measure of the amount of energy stored and amount of energy dissipated in the dielectric material due to an applied electric field, respectively. The real (ε_1) and imaginary (ε_2) parts of the complex permittivity for PAN nanofiber can be found using the equations [42]:

$$\varepsilon_1 = n^2 - k^2 \tag{13}$$

and

$$\varepsilon_2 = 2nk \tag{14}$$

Fig. 9 characterizes the wavelenght dependence of ε_1 and ε_2 of PAN nanofiber. Both the ε_1 and ε_2 values decrease with increasing the wavelenght for the PAN nanofiber. According to the figure, the ε_1 spectrum has two peaks while the ε_2 spectrum has a one peak. In addition, a peak of the ε_2 of 1.12 appears at 280 nm. The ε_2 value decreases sharply between 280 nm and 700 nm. The value of the ε_1 decreases slightly in the ranging of 350–2000 nm. The values of ε_1 and ε_2 change 12.796-20.902 and 0.273-0.746 in UV-Vis region, respectively. The values of ε_1 and ε_2 of ACNF layer prepared by Dincer et al. [9] change 2.22-0.047 and 2.4-0.083 in UV-Vis region (400-700 nm),

respectively. Mahmoud et al. [33] reported that the values of real (ε_1) and imaginary (ε_2) parts of dielectric constant vary from 11.5 to 8.5 and 7.1 to 11.2 between 200 and 700 nm, respectively.

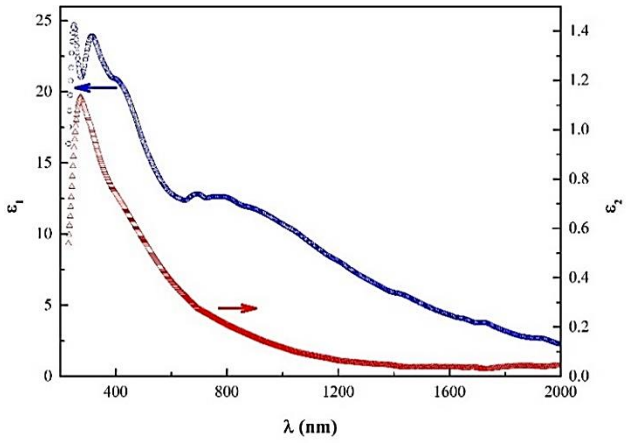

Fig. 9. Spectral dependence of the ε_1 and ε_2 of PAN Nanofibers (color online)

3.7. Dielectric loss tangent (tan δ) characteristics of PAN nanofiber

The dielectric loss tangent (tan δ) is due to the energy loss of specimen at a precise frequency, this parameter is found in terms of the imaginary and real the parts of the complex dielectric constant as follow [43]:

$$tan\delta = \frac{\varepsilon''}{\varepsilon'} \tag{15}$$

Fig. 10 characterizes the variation in the tan δ with photon energy for PAN nanofiber. It has been observed that tan δ increases with increasing photon energy and reaches a maximum. Then it decreases for further increase of photon energy. The spectrum of tan δ is defined by the presence of a peak at about 4.5 eV.

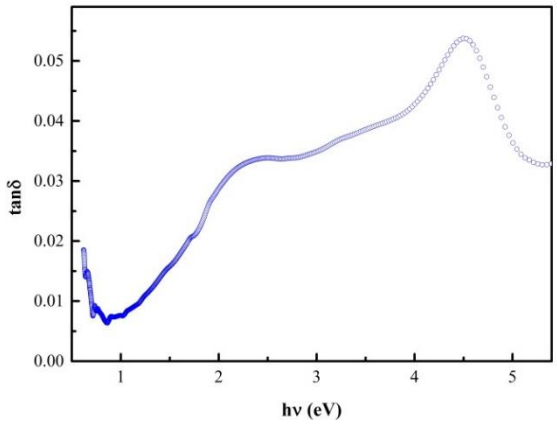

Fig. 10. Spectral dependence of the tan δ of PAN nanofibers (color online)

3.8. Optical conductivity caharacteristics of PAN film

The optical conductivity (σ_{opt}) directly depends on the refractive index (n) and absorption coefficient (α). The optical conductivity (σ) can be found using the following equation [44,45]:

$$\sigma_{opt} = \frac{\alpha nc}{4\pi} \tag{16}$$

where c is the velocity of light. Fig. 11 depicts the variation of the optical conductivity (σ_{opt}) with the photon energy ($h\upsilon$). It has been observed that σ_{opt} increases with increasing photon energy and reaches a maximum. Then it decreases for further increase of photon energy. The spectrum of σ_{opt} is characterized by the presence of a peak at about 4.63 eV. The value of peak is found to be 6.26 x10^{14} s^{-1}. The peak origin in σ_{opt} may be referred to the optical interband transitions [46].

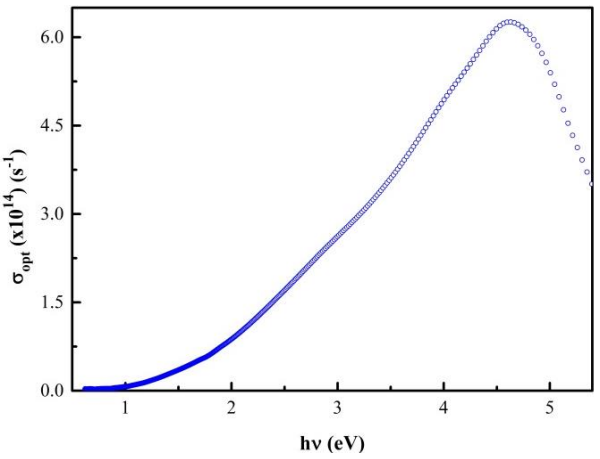

Fig. 11. The variation of the optical conductivity (σ_{opt}) with the photon energy ($h\upsilon$) for PAN nanofibers (color online)

3.9. Volume energy loss and surface energy loss of PAN nanofiber

The dielectric functions are used to evaluate the surface (S_{EL}) and volume (V_{EL}) energy loss functions [47,48]. These quantities are proportional to the characteristic energy loss of free charge carriers moving in the surface and interior of the films, respectively. The S_{EL} and V_{EL} energy loss functions can be determined using the following equations [47-49]

$$V_{EL} = Im\left(-\frac{1}{\varepsilon^*}\right) = \frac{\varepsilon''}{\varepsilon'^2+\varepsilon''^2} \tag{17}$$

and

$$S_{EL} = Im\left(-\frac{1}{\varepsilon^*+1}\right) = \frac{\varepsilon''}{(\varepsilon'+1)^2+\varepsilon''^2} \tag{18}$$

The values of V_{EL} and S_{EL} are found according to real and imaginary parts of the dielectric constant. This values

as a function of photon energy are illustrated in Fig. 12. As can be seen in Fig. 12 that the values of S_{EL} are higher than the V_{EL} of PAN nanofibers especially after 2 eV and the variation of V_{EL} follows the same trend as S_{EL}.

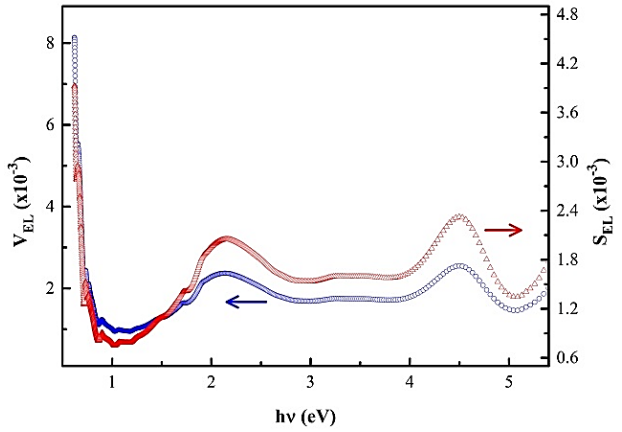

Fig. 12. The surface (S_{EL}) and volume (V_{EL}) energy loss functions with the photon energy (hυ) for PAN nanofibers (color online)

4. Conclusions

PAN nanofibres were fabricated from solution using electrospinning. The current study makes significant supports to fabrication of PAN nanofibers via eco-friendly, economical and easy electrospinning method. It has been investigated for the first time the optical and dispersion properties of PAN nanofibers for optoelectronic device applications. Furthermore, PAN nanofibers have homogeneous atomic distribution and good crystallinity.

The dielectric, optical parameter and dispersion properties of PAN nanofibers are interpreted from the reflectance and transmittance measurements achieved over the spectral area between 200 and 2000 nm. It is found that the value of optical band gap of direct transition for PAN nanofiber layer is 3.55 eV using Tauc's curve. The dispersion parameters were determined according to single oscillator model. On the basis of dielectric calculations, some of the optical constants of PAN nanofibers were evaluated.

On the basis of our results the optical dispersion and absorption work for PAN nanofibers let argument for the feasibility of PAN nanofibers in the area of photon energy applications.

References

[1] T. Tański, W. Matysiak, L. Markovicova, N. Florek-Szotowicz, P. Snopiński, Ł. Krzemiński, M. Wiśniowski, J. Achieve. Mater. Manuf. Eng. **73**(2), 176 (2015).
[2] T. Tański, W. Matysiak, Ł. Krzemiński, Mater. Manuf. Process. **32**(11), 1218 (2017).
[3] Z. Zhang, F. Zhang, X. Jiang, Y. Liu, Z. Guo, J. Leng, Fibers and Polymers **15**(11), 2290 (2014).
[4] H. Hou, J.J. Ge, J. Zeng, Q. Li, D. H. Reneker, A. Greiner, S. Z. D. Cheng, Chem. Mater. **17**, 967 (2005).
[5] T. Subbiah, G.S. Bhat, R.W. Tock, S. Parameswaran, S. S. Ramkumar, J. Appl. Polym. Sci. **96**, 557 (2005).
[6] K. Jayaraman, M. Kotaki, Y. Zhang, X. Mo, S. Ramakrishna, J. Nanosci. Nanotechnol. **4**, 52 (2004).
[7] J. J. Mack, L. M. Viculis, A. Ali, R. Luoh, G. Yang, H. T. Hahn, F. K. Ko, R.B. Kaner, Adv. Mater. **17**, 77 (2005).
[8] F. K. Ko, M. Gandhi, C. Karatzas, in: Proceedings of the 19th American Society for Composites Annual Technical Conference, Atlanta, GA, October 17-20, (2004).
[9] K. Dincer, B. Waisi, G. Önal, N. Tuğluoğlu, J. McCutcheon, Ö. F. Yüksel, Synth. Met. **237**, 16 (2018).
[10] O. P. Bahl, L. M. Manocha, Carbon **12**(4), 417 (1974).
[11] O. P. Bahl, R. B. Mathur, Fiber Sci. Technol. **12**(1), 31 (1979).
[12] Z. Wangxi, L. Jie, W. Gang, Carbon **41**(14), 2805 (2003).
[13] M. S. A. Rahaman, A. F. Ismail, A. Mustafa, Polym. Degrad. Stabil. **92**(8), 1421 (2007).
[14] J. C. Chen, I. R. Harrison, Carbon **40**(1), 25 (2002).
[15] M. C. Yang, D. C. Yu, Appl. Polym. Sci. **59**, 1725 (1996).
[16] E. Pamula, G. P. Rouxhet, Carbon **41**(10), 1905 (2003).
[17] Y. Wang, S. Serrano, J. J. Santiago-Aviles, Synth. Met. **138**, 423 (2003).
[18] S. Y. Gu, J. Rena, Q. L. Wu, Synth. Met. **155**, 157 (2005).
[19] S. H. Park, C. Kim, Y. O. Choi, K. S. Yang, Carbon **41**, 2655 (2003).
[20] S. Dadvar, H. Tavanai, M. Morshed, J. Nanopart. Res. **13**, 5163 (2011).
[21] J. S. Prasad, V. Dhand, V. Himabindu, Y. Anjaneyul, Int. J. Hydrogen Energ. **36**, 11702 (2011).
[22] S. Khan, J. A. Harsh, M. Husain, M. Zulfequar, Physica E **81**, 320 (2016).
[23] J. C. Manifacier, J. Gasiot, J. P. Fillard, J. Phys. **E9**, 1002 (1976).
[24] J. I. Pankove, Optical Processes in Semiconductors, Prentice Hall, NJ, (1971).
[25] A. A. M. Farag, I. S. Yahia, F. Yakuphanoğlu, M. Kandaz, W. A. Farooq, Opt. Commun. **285**, 3122 (2012).
[26] M. Çağlar, S. Ilıcan, Y. Çağlar, Thin Solid Films **517**, 5023 (2009).
[27] J. Tauc, Amorphous and liquid semiconductors, Plenum, New York, (1974).
[28] H. M. Zeyada, M. M. EL-Nahass, S. A. Samak, J. Non-Cryst. Solids **358**,915 (2012).
[29] A. A. M. Farag, S. M. S. Haggag, M. E. Mahmoud, Spectrochim. Acta Part A **82**, 467 (2011).
[30] W. Matysiak, T. Tański, P. Jarka, M. Nowak,

M. Kępińska, P. Szperlich, Opt. Mater. **83**, 45 (2018).
[31] D. Singh, S. Kumar, R. Thangaraj, J. Non-Cryst. Solids **358**, 2826 (2012).
[32] A. A. M. Farag, M. Fadel, Opt. Laser Technol. **45**, 356 (2013).
[33] W. E. Mahmoud, F. S. Al-Hazmi, A. A. Al-Ghamdi, F. S. Shokr, G. W. Beall, L.M. Bronstein, Superlattice Microst. **96**, 174 (2016).
[34] F. Urbach, Phys. Rev. **92**, 1324 (1953).
[35] A. F. Qasrawi, Cryst. Res. Technol. **40**, 610 (2005).
[36] S. H. Wemple, M. Didomenico, Jr., Phys. Rev. Lett. **23**, 1156 (1969).
[37] S. H. Wemple, M. Didomenico, Jr., Phys. Rev. **B3**, 1338 (1971).
[38] A. A. M. Farag, I. S. Yahia, Opt. Commun. **283**, 4310 (2010).
[39] M. M. El-Nahass, A. A. Atta, E. A. A. El-Shazly, A. S. Faidah, A. A Hendi, Mater. Chem. Phys. **117**, 390 (2009).
[40] F. Yakuphanoglu, A. Cukurovali, I. Yilmaz, Physica B **353**, 210 (2004).
[41] M. Çaglar, S. Ilıcan, Y. Calgan, Y. Şahin, F. Yakuphanoglu, D. Hur, Spectrochim. Acta A **71**, 621 (2008).
[42] A. A. M. Farag, I. S. Yahia, Opt. Commun. **283**, 4310 (2010).
[43] W. M. Desokya, Mahmoud S. Dawooda, M. M. El-Nahass, Optik-Int. J. for Light and Electron Optics **178**, 351 (2019).
[44] J. I. Pankove, Optical Processes in Semiconductors, Dover, New York, (1975).
[45] D. Singh, S. Kumar, R. Thangaraj, J. Non-Cryst. Solids **358**, 2826 (2012).
[46] F. Yakuphanoğlu, M. Şekerci, O. F. Öztürk, Opt. Commun. **239**, 275 (2004).
[47] A. M. Adama, E. Lilov, E. M. M. Ibrahim, P. Petkov, L. V. Panina, M. A. Darwish, J. Mater. Process. Technol. **264**, 76 (2019).
[48] Ezzat El-Sayed, Hamed, Appl. Surf. Sci. **250**, 70 (2005).
[49] A. Bagheri Khatibani, S. M. Rozati, J. Non-Cryst. Solids **363**, 121 (2013).

* Corresponding author: fyuksel@selcuk.edu.tr